SIMULATION AND EXTRA SHORT–TERM FORECAST OF WIND CHARACTERISTICS FROM THE DATA OF LIDAR WIND SOUNDING

V.S. Komarov, V.I. Akselevich, A.I. Grishin, A.V. Kreminskii, N.Ya. Lomakina, and G.G. Matvienko

Institute of Atmospheric Optics,
Siberian Branch of the Russian Academy of Sciences, Tomsk
Received January 12, 1995

In this paper we consider the local empirical model of wind for the atmospheric boundary layer, constructed based on the measurement data obtained with a three–path correlation lidar. The quality of extra short–term forecast of zonal and meridional wind using MMCA is evaluated.

Nowadays the lidar wind sounding is gaining progressively wide acceptance in modern meteorology (see, e.g., Refs. 1–3). The use of lidar wind sounding data for studying the wind field opens new opportunities for detailed investigation into the atmospheric circulation within the boundary layer (1–2 km altitude range). This is because the results of lidar wind sounding are characterized by high spatiotemporal resolution and by the accuracy quite suitable for practical purposes (for evaluation of the accuracy see Refs. 2, 4, and 5) in contrast to the radiosonde data characterized by a low reliability due to very fast rise of radiosondes about 150–300 m/min, low height resolution, and low frequency of observations (no more than four times a day). This is important not only in studying the local structure of the wind field in the low atmosphere but in solving the problems of atmospheric ecological monitoring, particularly, the problems of diagnostics and forecast of spatial propagation of anthropogenic atmospheric emissions, which is governed largely by the state of wind regime. It is clearly seen from the equation of such emission transfer, which can be written in the form[6,7]

$$\frac{\partial s}{\partial t} = -\left(u\frac{\partial s}{\partial x} + v\frac{\partial s}{\partial y}\right) - w\frac{\partial s}{\partial z} - \frac{\partial w_a s}{\partial z} +$$

$$+ k_p\left(\frac{\partial^2 s}{\partial x^2} + \frac{\partial^2 s}{\partial y^2}\right) + \frac{\partial}{\partial z}k\frac{\partial s}{\partial z} - \varepsilon_a , \qquad (1)$$

where s is the concentration of an impurity in the emission; t is the time; u, v, and w are the horizontal and vertical wind velocity components along x, y, and z axes; w_a is the vertical velocity of an impurity a; $k_p = k_x = k_y$ and k are the eddy diffusion coefficients; $\varepsilon_a = \varepsilon_a(x, y, z, t)$ is the source (sink) of an impurity a.

It should be emphasized here that according to Ref. 8 the vector of horizontal motion of a particle from the emission source to the point of fall onto the ground, s, is proportional to the integral of the wind velocity vector over the vertical, i.e.,

$$s \sim \frac{1}{h}\int_0^h \mathbf{v}(z)\,\mathrm{d}z , \qquad (2)$$

where h is the height of fall of an impurity. Therefore, in practice the calculations of a pollution cloud spread normally use zonal and meridional wind components averaged over vertical layers $h - h_0$ (at $h_0 = 0$) or, in other words, the vector of the mean wind[8,9]

$$\langle \mathbf{v} \rangle_{0,\,h} = \frac{1}{h}\int_0^h \mathbf{v}(z)\,\mathrm{d}z . \qquad (3)$$

With regard to the above said, the authors have attempted, based on the data of lidar wind sounding, to construct local empirical model of wind for the boundary atmospheric layer and to evaluate the quality of the extra short–term (with the predictability of 4 to 12 hr) forecast of zonal and meridional components of mean wind vector. The forecast has been done using the modified method of clustering of arguments[10] (MMCA) which was shown in Refs. 9 and 11 to be sufficiently simple and not needed for a large bulk of initial information for constructing optimal prognostic models. The subject of the present paper are the results of numerical experiments on simulation and forecasting of wind characteristics based on the data of lidar sounding.

We performed the aforementioned numerical experiments based on the data of routine field observations about the wind obtained with a three–path correlation lidar (for its detailed description see Ref. 12) in Tomsk (56°N, 85°E) region from July 10 till August 12, 1994. A total of 90 six–time (at 2, 6, 10, 14, 18, and 22 hours, local time) observations about the wind profile in 140–1140 m altitude layer with the spatial resolution of 100 m was used. This allowed us to study the vertical structure of the wind field in the boundary atmospheric layer (up to 1140 m altitude). As to the algorithm of MMCA used for forecasting, we omit its description in this paper since it can be found in Refs. 11 and 13.

It should be finally noted that the local empirical model of wind, discussed below, includes the vertical profiles of the mean values ($\overline{\xi}$) and standard (rms) deviations (σ_ξ) of zonal (U) and meridional (V) wind, as well as the corresponding correlation matrices $||R_U||$ and $||R_V||$. At the same time the accuracy of forecasting the mean wind vector characteristics is estimated using rms deviations (E) of precalculated values of components $\langle U \rangle$ and $\langle V \rangle$ from the corresponding measured values and the probability of their discrepancy less than ±1 … ± 4 m/s and greater than ±4 m/s.

0235-6880/95/07 539-05 $02.00

Consider now the results of numerical experiments on simulation and forecasting of wind characteristics based on the data of lidar wind sounding and first of all the results of constructing the local empirical model. To do this, let us use Figs. 1 and 2, where the mean values and standard deviations for daytime, nighttime, and in the mean for 24–hour period are presented.

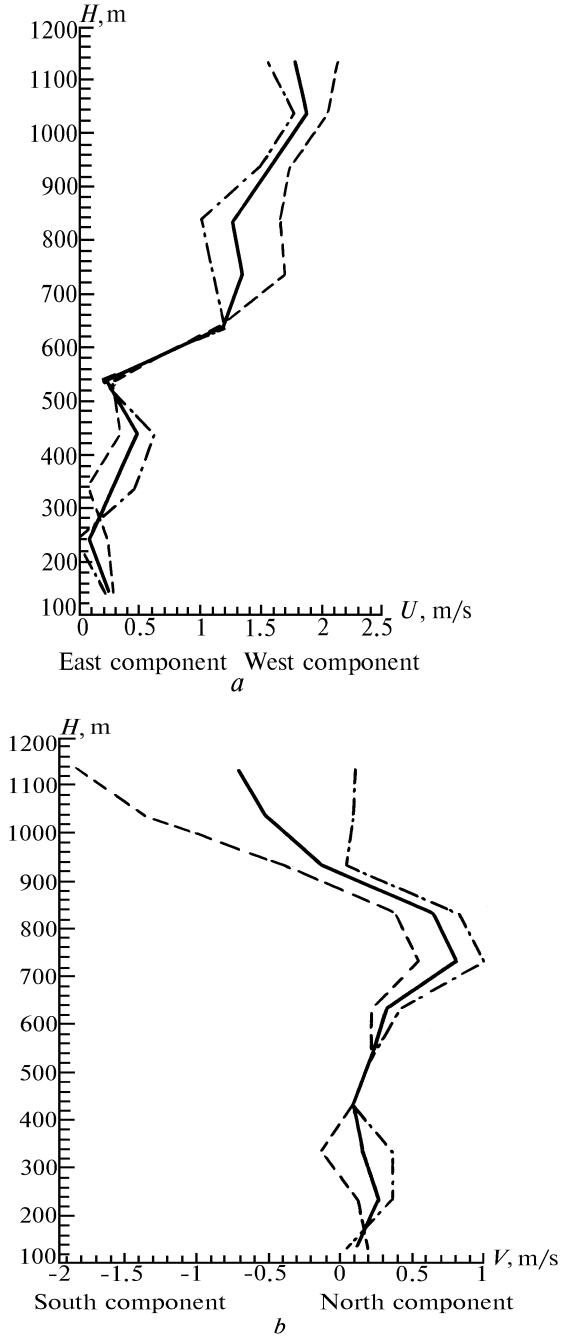

FIG. 1. Altitude distribution of mean velocity of zonal (a) and meridional (b) wind: average daily profile (solid line), daytime profile (dot–and–dash line), and nighttime profile (dashed line).

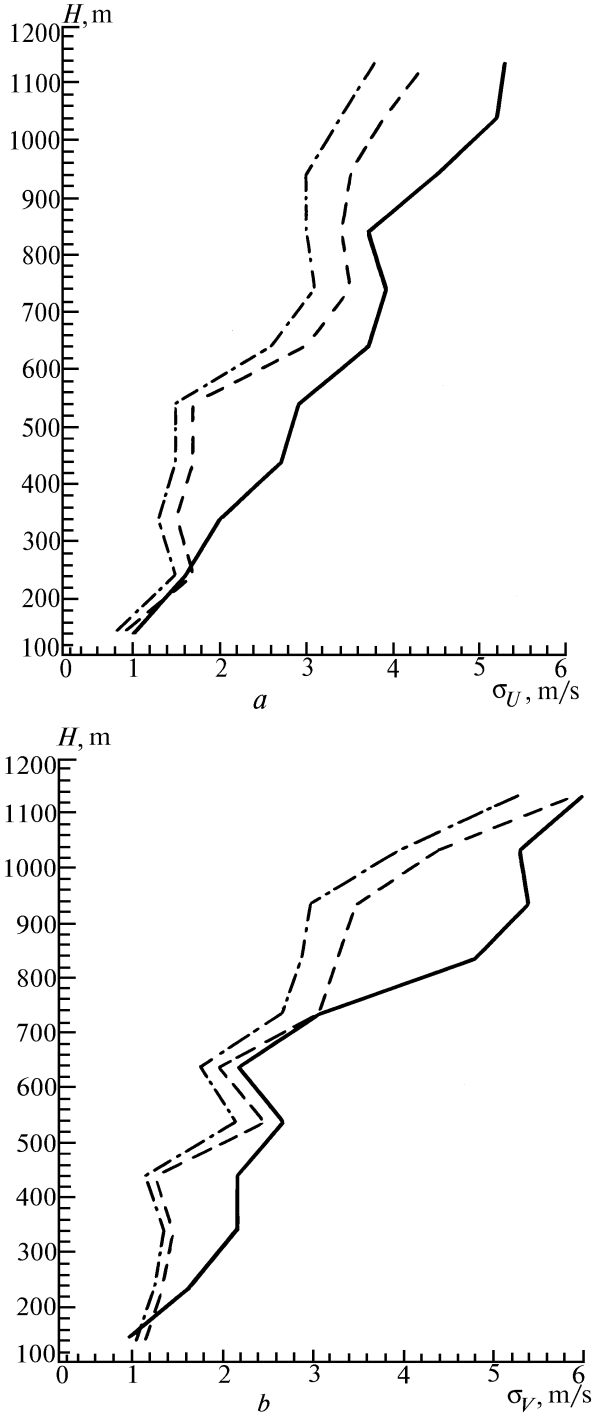

FIG. 2. Altitude distribution of standard deviations of zonal (a) and meridional (b) wind velocity: average daily profile (solid line), daytime profile (dot–and–dash line), and nighttime profile (dashed line).

Analysis of the above figures shows that:

1) In summer the boundary layer is characterized by small (not greater than ±2 m/s) mean values of zonal and meridional wind velocities which are practically constant at

altitude up to 550 and 650 m, respectively. Above these levels and after some maximum at the altitude of 750 m the marked strengthening of zonal and especially meridional wind is observed.

2) In contrast to zonal wind, the diurnal amplitude (i.e., difference between day and night values) of the meridional wind velocity markedly increases at altitudes above 850 m and it reaches 2 m/s at the altitude of 1100 m.

3) At altitudes above 850 m it is typical for meridional wind that it changes its sign (direction): the northern wind observed during the day changes to the southern one overnight.

4) The vertical distribution of standard deviations of zonal and meridional wind velocity possesses a pronounced altitude–dependence, being about 1 m/s near the ground and 5–6 m/s at the altitude of 1100 m.

The model description of vertical statistical structure of the wind field is not comprehensive if we do not consider the peculiarities of autocorrelation connections of this meteorological parameter. This should also be done because reliable enough data on peculiarities of wind interlevel connections in the boundary layer are not yet available, since the data of radiosonde measurements do not allow their detailed evaluation because of the low altitude resolution. With regard to the aforementioned facts calculated on the basis of lidar wind sounding data are also the correlation matrices providing more comprehensive information about vertical structure of zonal and meridional wind velocity variations within the boundary layer. These matrices are tabulated in Table I.

As is seen from Table I, weak interlevel correlation is typical for both zonal and meridional wind at low altitude (140–240 m). At the upper levels sufficiently higher correlation coefficients are observed, moreover, the interlevel connections increase with increasing wind velocity.

The second part of the present paper is devoted to extra short–term forecast (with predictability of 4–12 h) of zonal and meridional wind using modified version of MCA. As the initial statistical sample we use 11 profiles of vertical distribution of zonal and meridional wind (according to Ref. 9, it is the optimal number in terms of the forecast quality) as well as their values in 140–240 m layer at the time of observation. The choice of this layer is accounted for by the peculiarities of the wind lidar, whose ability to operate falls off under conditions of cloudiness, especially cumulus.[5] Having information from altitudes below the lower boundary of cloudiness, we can reconstruct the values of zonal and meridional wind at upper levels reliably enough.

The vertical distribution of zonal and meridional wind was forecasted for time periods of 4, 8, and 12 h. In numerical experiment, 50 vertical profiles with time period of forecast shorter than 4 h, 42 profiles with time period shorter than 8 h, and 30 profiles with time period shorter than 12 h were reconstructed. The quality of the forecast was evaluated using rms error E and probability P of errors (discrepancies between reconstructed values $\langle U \rangle$ and $\langle V \rangle$ and corresponding actual values) less than ±1 … ±4 m/s and greater than ±4 m/s.

Let us then consider the results of numerical experiments tabulated in Tables II–IV, where the results of statistical evaluation of the forecast quality for altitude structure of wind fields for the periods of 4, 8, and 12 h.

TABLE I. Autocorrelation matrices of zonal and meridional wind velocity constructed on the basis of data of lidar wind sounding.

Level, m	140	240	340	440	540	640	740	840	940	1040	1140
Zonal wind											
140	1.00	0.24	0.07	0.15	0.05	0.39	0.36	0.26	0.23	0.21	0.19
240	0.24	1.00	0.13	0.04	0.02	0.17	0.11	0.30	0.27	0.23	0.14
340	0.07	0.13	1.00	0.65	0.43	0.23	0.15	0.37	0.33	0.20	0.18
440	0.15	0.04	0.65	1.00	0.77	0.47	0.49	0.51	0.35	0.07	0.04
540	0.05	0.02	0.43	0.77	1.00	0.54	0.54	0.43	0.13	− 0.11	− 0.18
640	0.39	0.17	0.23	0.47	0.54	1.00	0.85	0.65	0.44	0.19	0.16
740	0.36	0.11	0.15	0.49	0.54	0.85	1.00	0.56	0.28	0.07	0.09
840	0.26	0.30	0.37	0.51	0.43	0.65	0.56	1.00	0.62	0.48	0.37
940	0.23	0.27	0.33	0.35	0.13	0.44	0.28	0.62	1.00	0.80	0.64
1040	0.21	0.23	0.20	0.07	− 0.11	0.19	0.07	0.48	0.80	1.00	0.76
1140	0.19	0.14	0.18	0.04	− 0.18	0.16	0.09	0.37	0.64	0.76	1.00
Meridional wind											
140	1.00	−0.02	0.00	0.12	0.10	0.15	0.30	0.26	0.28	0.38	0.38
240	−0.02	1.00	0.01	−0.03	−0.01	0.08	0.08	−0.09	−0.06	0.00	0.13
340	0.00	0.01	1.00	0.41	0.59	0.46	0.31	0.22	0.22	0.26	0.26
440	0.12	− 0.03	0.41	1.00	0.37	0.21	0.40	0.52	0.44	0.41	0.48
540	0.10	− 0.01	0.59	0.37	1.00	0.70	0.42	0.34	0.26	0.36	0.35
640	0.15	0.08	0.46	0.21	0.70	1.00	0.54	0.37	0.04	0.24	0.40
740	0.30	0.08	0.31	0.40	0.42	0.54	1.00	0.77	0.48	0.50	0.61
840	0.26	−0.09	0.22	0.52	0.34	0.37	0.77	1.00	0.56	0.47	0.59
940	0.28	−0.06	0.22	0.44	0.26	0.04	0.48	0.56	1.00	0.82	0.56
1040	0.38	0.00	0.26	0.41	0.36	0.24	0.50	0.47	0.82	1.00	0.82
1140	0.38	0.13	0.26	0.48	0.35	0.40	0.61	0.59	0.56	0.82	1.00

TABLE II. Standard errors E and probability (P) of errors of reconstruction of zonal and meridional wind velocity less than ±1 … ±4 m/s *and greater than* ±4 m/s, *obtained using MMCA from the data of wind lidar measurements in* 4–h *intervals.*

Layer of reconstruction, m	Probability, *P*					*E*
	≤ ± 1 m/s	≤ ± 2 m/s	≤ ± 3 m/s	≤ ± 4 m/s	> ± 4 m/s	
			Zonal wind			
140 – 340	0.92	1.00	1.00	1.00	0.00	0.6
140 – 440	0.84	0.98	1.00	1.00	0.00	0.8
140 – 540	0.80	0.90	0.98	1.00	0.00	1.0
140 – 640	0.80	0.92	0.96	1.00	0.00	1.1
140 – 740	0.76	0.92	0.96	0.98	0.02	1.2
140 – 840	0.80	0.90	0.96	0.98	0.02	1.3
140 – 940	0.78	0.92	0.96	0.96	0.04	1.3
140 – 1040	0.76	0.88	0.94	0.96	0.04	1.4
140 – 1140	0.64	0.88	0.94	0.96	0.04	1.5
			Meridional wind			
140 – 340	0.94	0.97	0.97	0.97	0.03	0.7
140 – 440	0.91	0.94	0.97	0.97	0.03	1.0
140 – 540	0.82	0.91	0.94	0.97	0.03	1.4
140 – 640	0.73	0.91	0.94	0.97	0.03	1.6
140 – 740	0.73	0.85	0.94	0.97	0.03	2.0
140 – 840	0.67	0.85	0.91	0.97	0.03	2.2
140 – 940	0.61	0.85	0.90	0.94	0.06	1.7
140 – 1040	0.61	0.85	0.85	0.88	0.12	2.0
140 – 1140	0.61	0.79	0.85	0.88	0.12	2.3

TABLE III. Standard errors E and probability (P) of errors of reconstruction of zonal and meridional wind velocity less than ±1 … ±4 m/s *and greater than* ±4 m/s, *obtained using MMCA from the data of wind lidar measurements in* 8–h *intervals.*

Layer of reconstruction, m	Probability *P*					*E*
	≤ ± 1 m/s	≤ ± 2 m/s	≤ ± 3 m/s	≤ ± 4 m/s	> ± 4 m/s	
			Zonal wind			
140 – 340	0.91	0.98	1.00	1.00	0.00	0.7
140 – 440	0.82	0.95	0.98	1.00	0.00	1.1
140 – 540	0.77	0.91	0.93	0.98	0.02	1.3
140 – 640	0.75	0.86	0.91	0.91	0.09	1.7
140 – 740	0.73	0.89	093	0.93	0.07	1.9
140 – 840	0.64	0.86	0.95	0.95	0.05	1.8
140 – 940	0.61	0.80	0.93	0.93	0.07	2.1
140 – 1040	0.55	0.84	0.91	0.93	0.07	2.1
140 – 1140	0.55	0.80	0.89	0.93	0.07	2.2
			Meridional wind			
140 – 340	0.86	0.96	0.98	1.00	0.00	0.8
140 – 440	0.84	.090	0.98	1.00	0.00	1.3
140 – 540	0.72	.088	0.94	0.98	0.02	1.6
140 – 640	0.70	0.84	0.92	0.94	0.06	1.8
140 – 740	0.68	0.82	0.84	0.94	0.06	2.2
140 – 840	0.66	0.78	0.82	0.92	0.08	2.4
140 – 940	0.62	0.80	0.84	0.90	0.10	1.9
140 – 1040	0.60	0.78	0.86	0.90	0.10	2.1
140 – 1140	0.58	0.76	0.82	0.88	0.12	2.3

TABLE IV. Standard errors E and probability (P) of errors of reconstruction of zonal and meridional wind velocity less than ±1 ... ±4 m/s *and greater than* ±4 m/s, *obtained using MMCA from the data of wind lidar measurements in* 12–h *intervals.*

Layer of reconstruction, m	Probability, P					E
	≤ ± 1 m/s	≤ ± 2 m/s	≤ ± 3 m/s	≤ ± 4 m/s	> ± 4 m/s	
			Zonal wind			
140 – 340	0.84	0.97	1.00	1.00	0.00	0.9
140 – 440	0.80	0.94	0.98	0.98	0.02	1.2
140 – 540	0.69	0.85	0.88	0.97	0.03	1.5
140 – 640	0.66	0.88	0.91	0.94	0.06	1.9
140 – 740	0.66	0.85	0.91	0.91	0.09	2.1
140 – 840	0.60	0.79	0.88	0.91	0.09	2.3
140 – 940	0.57	0.82	0.88	0.94	0.06	2.4
140 – 1040	0.57	0.82	0.88	0.91	0.09	2.5
140 – 1140	0.55	0.82	0.88	0.91	0.09	2.5
			Meridional wind			
140 – 340	0.82	0.93	0.95	0.98	0.02	1.0
140 – 440	0.80	0.86	0.91	0.93	0.07	1.6
140 – 540	0.70	0.82	0.86	0.89	0.11	1.9
140 – 640	0.64	0.77	0.84	0.89	0.11	2.2
140 – 740	0.64	0.82	0.84	0.86	0.14	2.3
140 – 840	0.59	0.80	0.84	0.86	0.14	2.3
140 – 940	0.59	0.82	0.91	0.93	0.07	2.0
140 – 1040	0.55	0.80	0.84	0.88	0.12	2.2
140 – 1140	0.57	0.73	0.76	0.84	0.16	2.3

As follows from the analysis of data presented in Tables II–IV, the forecast of vertical distribution of wind using the modified MCA is efficient enough, and for the forecast with the 4–h time high values of the probability ($P > 0.6$) of errors less than ±1 m/s are characteristic of the entire layer under study. With increasing time of forecast, its quality somewhat reduces, and for 12–h forecast high values of the probability are observed only in 140–740 m layer for both zonal and meridional wind.

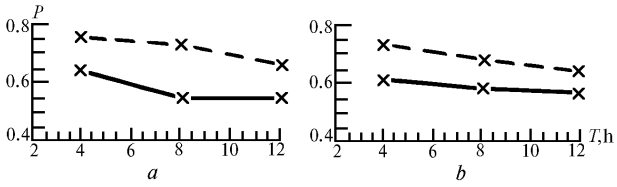

FIG. 3. Probability P of errors of forecast of zonal (a) and meridional (b) wind less than ±1 m/s *vs. interval between lidar observations: for* 140–1140 m *layer (solid line) and for* 140–740 m *layer (dashed line).*

So we can conclude that modified MCA can be used for solving the problems on reconstruction of vertical distribution of wind, the main factor of atmospheric pollution transport, in the boundary atmospheric layer, but to do this the intervals between wind lidar measurements must be shorter than 6–7 h (Fig. 3). At the same time, for the lower part of the boundary atmospheric layer (0–740 m) the interval between measurements may be up to 12 h.

In conclusion it should be noted that above conclusions are tentative, since the simulation and forecast of wind were performed based on experimental data of only one season (summer) of 1994. To check and refine the obtained results, we naturally need a more long series of lidar wind sounding.

REFERENCES

1. V.E. Zuev and V.V. Zuev, *Remote Optical Sounding of the Atmosphere* (Gidrometeoizdat, St. Petersburg, 1992), 232 pp.
2. A.I. Grishin, A.E. Zil'berman, and G.G. Matvienko, in: *Abstracts of Reports at the First Inter–Republic Symposium on Atmospheric and Ocean Optics*, Tomsk, 1994, Vol. 2, pp. 36–37.
3. R.M. Hardesty, et al., in: *14th ILRC*, San Candido, 20–24 June, 1988, pp. 440–443.
4. V.S. Komarov, V.I. Akselevich, A.V. Kreminskii, and G.G. Matvienko, Atmos. Oceanic Opt. **7**, No. 2, 96–99 (1994).
5. B.D. Belan, G.G. Matvienko, A.I. Grishin, et al., Atm. Opt. **4**, No. 10, 746–749 (1991).
6. P.N. Belov and V.S. Komarov, Atmos. Oceanic Opt. **7**, No. 2, 103–107 (1994).
7. A.M. Vladimirov, Yu.I. Lyakhin, L.T. Matveev, and V.G. Orlov, *Environmental Protection* (Gidrometeoizdat, Leningrad, 1991), 423 pp.
8. F.F. Bryukhan', *Methods for Climatic Procession and Analysis of Aerological Information* (Gidrometeoizdat, Moscow, 1991), 112 pp.
9. V.S. Komarov, V.I. Akselevich, and A.V. Kreminskii, Atmos. Oceanic Opt. **7**, No. 2, 125–128 (1994).
10. Yu.L. Kocherga, Avtomatika, No. 5, 80–87 (1991).
11. V.S. Komarov, V.I. Akselevich, and A.V. Kreminskii, Atmos. Oceanic Opt. **7**, No. 2, 121–124 (1994).
12. G.G. Matvienko, G.O. Zadde, E.S. Ferdinandov, et al., *Correlation Methods of Lidar Wind Measurements* (Nauka, Novosibirsk, 1985), 221 pp.
13. V.S. Komarov and A.V. Kreminskii, Atmos. Oceanic Opt. **8**, No. 7, 488–495 (1994).